Bioelectromagnetics 30:489–499 (2009)

Low-Frequency Conductivity Tensor of Rat Brain Tissues Inferred From Diffusion MRI

Masaki Sekino,[1]* Hiroyuki Ohsaki,[1] Sachiko Yamaguchi-Sekino,[2] Norio Iriguchi,[3] and Shoogo Ueno[4]

[1]*Department of Advanced Energy, Graduate School of Frontier Sciences, The University of Tokyo, Tokyo, Japan*
[2]*Department of Biomedical Engineering, Graduate School of Medicine, The University of Tokyo, Tokyo, Japan*
[3]*Center for Multimedia and Information Technologies, Kumamoto University, Kumamoto, Japan*
[4]*Department of Applied Quantum Physics, Graduate School of Engineering, Kyushu University, Fukuoka, Japan*

Conductivity tensor maps of the rat brain were obtained using diffusion magnetic resonance imaging (MRI). Signal attenuations in the cortex and the corpus callosum were measured using the stimulated echo acquisition mode (STEAM) sequence with b factors up to 6000 s/mm^2. Our previously published method was improved to infer 3×3 conductivity tensor at the low-frequency limit. The conductivity tensor of the tissue was inferred from the fast component of the diffusion tensor and a fraction of the fast component. The mean conductivity (MC) of the cortex and the corpus callosum was 0.52 and 0.62 S/m, respectively. Diffusion-weighted images were obtained with b factors up to 4500 s/mm^2. Conductivity tensor images were calculated from the fast diffusion tensor images. Tissues with highly anisotropic cellular structures, such as the corpus callosum, the internal capsule, and the trigeminal nerve, exhibited high anisotropy in conductivity. The resulting values corresponded to conductivities at the low-frequency limit because our method assumed electric currents flowing only through extracellular fluid. Bioelectromagnetics 30:489–499, 2009.

Key words: conductivity; magnetic resonance

INTRODUCTION

The imaging of conductivity distributions could give valuable information on physiological and pathological parameters, which are not obtained by anatomical imaging. For example, conductivity measurements can be used to classify different tissue types [Mayer et al., 2006], and to find edema in tissues [Merwa et al., 2004]. Electrical impedance tomography (EIT), in which surface potentials are measured during applications of currents via surface electrodes, has been applied to obtain conductivity distributions in living bodies [Matherall et al., 1996; Saulnier et al., 2001]. However, EIT has relatively low spatial resolution when using a limited number of surface electrodes. Moreover, conductivity distributions of the brain are difficult to obtain because most of the currents do not penetrate the skull due to its low conductivity [Sekino and Ueno, 2002]. Some new methods use magnetic resonance imaging (MRI) to obtain conductivity distributions. Conductivity-weighted images are obtained during applications of external oscillating magnetic fields, which induce conductivity-dependent eddy currents in a sample [Ueno and Iriguchi, 1998; Yukawa et al., 1999].

Low-frequency electric currents in living tissues are mainly conducted by migrations of ions. Conductivity is inversely proportional to the viscosity of water because the viscous resistance acting on migrating ions is proportional to the viscosity of water. The

Grant sponsor: Ministry of Education, Culture, Sports, Science and Technology, Japan; Gran-in-Aid for Young Scientists(A) (No. 18680037) and Grant-in-Aid for Scientific Research(s) (No. 17100006).

*Correspondence to: Masaki Sekino, Transdisciplinary Sciences Building 312, 5-1-5 Kashiwanoha, Chiba 277-8561, Japan.
E-mail: sekino@k.u-tokyo.ac.jp

Received for review 30 October 2008; Final revision received 30 March 2009

DOI 10.1002/bem.20505
Published online 12 May 2009 in Wiley InterScience (www.interscience.wiley.com).

self-diffusion coefficient of water is also inversely proportional to the viscosity of water, which is known as the Stokes–Einstein equation. These relations suggest that the conductivity tensor is, in principle, a scaling of the water self-diffusion tensor. The scaling relation between the self-diffusion coefficient of water and conductivity has been investigated in microemulsions [Xu et al., 2001; Kataoka et al., 2003] and multiphase ceramics [Kreuer et al., 1994]. Changes in the apparent diffusion coefficient (ADC) of water and conductivity are correlated in tissues under acute cerebral ischemia [Verheul et al., 1994]. Since the migrating ions encounter high resistance from cell membranes, most of the currents flow through extracellular fluid. We obtained the ADCs and fractions of intra/extracellular spaces from the relation between the signal intensity of diffusion-weighted images and the *b* factor of motion-probing gradients (MPGs), and calculated conductivity images of the rat brain [Sekino et al., 2003] and the human brain [Sekino et al., 2005]. This method requires neither an injection of electric current nor a prior measurement of conductivity. However, these conductivity measurements were limited to three orthogonal directions, or to a two-dimensional tensor. More recently, Wang et al. [2008] proposed another method to estimate conductivity from diffusion tensor MRI, though the application of this method is limited to white matter tissues.

In this article, magnetic resonance signals in the cortex and the corpus callosum were obtained using the stimulated echo acquisition mode (STEAM) sequence, and tissue conductivities were calculated from the signals. The *b* factor was arrayed in 61 steps to improve the accuracy of estimations of conductivities and the fractional volumes of intra/extracellular spaces. In addition, diffusion-weighted images were obtained with applications of MPGs in six directions to construct 3×3 conductivity tensor images.

THEORY

The effective conductivity (σ) of tissue can be calculated using the following equation on the assumption that all the currents flow through extracellular fluid [Cole et al., 1969]:

$$\sigma = \frac{2v_{\mathrm{ext}}\sigma_{\mathrm{ext}}}{3 - v_{\mathrm{ext}}} \tag{1}$$

where v_{ext} is the fractional volume of extracellular space and σ_{ext} is the conductivity of the extracellular fluid. The conductivity (σ_{ext}) and the diffusion coefficient in the extracellular fluid (D_{ext}) are related by the following equation which has been derived from the balance between the electrostatic force and the viscous resistance acting on migrating ions [Sekino et al., 2003]

$$\sigma_{\mathrm{ext}} = \frac{r_{\mathrm{w}} q^2 N}{r_i kT} D_{\mathrm{ext}} \tag{2}$$

where r_{w} is the Stokes radius of a water molecule, r_i is the Stokes radius of an ion, q is the charge of the ion, N is the density of the ion, k is the Boltzmann constant, and T is the absolute temperature.

The signal intensity of diffusion MRI is given by the following equation for samples having anisotropic diffusion of water:

$$S_i = f \exp(-b\mathbf{g}_i^{\mathrm{T}}\mathbf{D}\mathbf{g}_i) \tag{3}$$

where f is a coefficient, S_i is the signal intensity measured with an MPG direction i (in this article, $i = 1, 2, \ldots, 6$), $\mathbf{g}_i$ is a unit vector representing the MPG direction, and $\mathbf{D}$ is the diffusion tensor. The attenuation factor b is defined as $b = \gamma^2 G^2 \delta^2 (\Delta - \delta/3)$, where γ is the gyromagnetic ratio, G is the gradient intensity, δ is the duration of MPGs, and Δ is the interval between the leading edges of MPGs. Recent studies on diffusion MRI indicate that the diffusion signal attenuation significantly deviates from monoexponential decay at high b values (up to 4000 s/mm^2 or more) [Niendorf et al., 1996; Clark and Le Bihan, 2000; Clark et al., 2002; Sano et al., 2003; Maier et al., 2004]. In this case, the signal attenuation is better described in terms of a biexponential function representing two water diffusion compartments with fast and slow diffusion tensors:

$$S_i = f_{\mathrm{fast}} \exp(-b\mathbf{g}_i^{\mathrm{T}}\mathbf{D}_{\mathrm{fast}}\mathbf{g}_i) + f_{\mathrm{slow}} \exp(-b\mathbf{g}_i^{\mathrm{T}}\mathbf{D}_{\mathrm{slow}}\mathbf{g}_i) \tag{4}$$

where $\mathbf{D}_{\mathrm{fast}}$ and $\mathbf{D}_{\mathrm{slow}}$ are the fast and slow components of the diffusion tensor, and f_{fast} and f_{slow} are the fractions of the fast and slow components. Though an interpretation of the origins of the two components has not yet been established, in some studies, the fast component and the slow component have been attributed to extracellular fluid and intracellular fluid, respectively, based on experimental results [Niendorf et al., 1996; Sano et al., 2003].

The conductivity tensor $\mathbf{C}$ is defined as a 3×3 symmetric matrix

$$\mathbf{C} = \begin{pmatrix} \sigma_{xx} & \sigma_{\mathrm{xy}} & \sigma_{\mathrm{zx}} \\ \sigma_{xy} & \sigma_{\mathrm{yy}} & \sigma_{\mathrm{yz}} \\ \sigma_{zx} & \sigma_{\mathrm{yz}} & \sigma_{\mathrm{zz}} \end{pmatrix} \tag{5}$$

The conductivity tensor $\mathbf{C}$ is quantitatively inferred from the fast diffusion tensor ($\mathbf{D}_{\mathrm{fast}}$) and the fraction

of the fast component (f_{fast}) by the following equation [Sekino et al., 2003]:

$$\mathbf{C} = \frac{2f_{\text{fast}}}{3 - f_{\text{fast}}} \frac{r_w q^2 N}{r_i kT} \mathbf{D}_{\text{fast}} \tag{6}$$

This equation was derived on the assumption that the diffusion coefficient and the fractional volume of extracellular fluid are equal to the fast component of the ADC and the fraction of the fast component ($D_{\text{ext}} = \mathbf{g}_i^{\text{T}} \mathbf{D}_{\text{fast}} \mathbf{g}_i$, $v_{\text{ext}} = f_{\text{fast}}$). Though extracellular fluid is a complicated electrolyte containing various ions and macromolecules, we assume for simplicity that the composition of extracellular fluid is equal to that of a saline solution (0.15 mol/L NaCl) [Geddes and Baker, 1967]. Based on this assumption, the constants in Equation (6) are $r_w/r_i = 0.76$, $q = 1.6 \times 10^{-19}$ C, $N = 1.8 \times 10^{26}\,\text{m}^{-3}$, and $kT = 4.3 \times 10^{-21}$ J [Atkins, 1998]. These values lead to the following equation:

$$\mathbf{C} = \frac{2f_{\text{fast}} \times (8.1 \times 10^8 [\text{S s/m}^3])}{3 - f_{\text{fast}}} \mathbf{D}_{\text{fast}} \tag{7}$$

Since the 3×3 conductivity tensor has six independent elements, a minimum of six MPG directions is necessary to completely determine the conductivity tensor. Several gradient direction sets with six or more gradient directions have been proposed that cover space more efficiently, benefiting tensor measurements [Jones et al., 1999; Papadakis et al., 1999; Hasan et al., 2001]. In this study, MPGs are applied in the following six directions: $\mathbf{g}_1 = (1/\sqrt{2})(1\,0\,1)^{\text{T}}$, $\mathbf{g}_2 = (1/\sqrt{2})(-1\,0\,1)^{\text{T}}$, $\mathbf{g}_3 = (1/\sqrt{2})(0\,1\,1)^{\text{T}}$, $\mathbf{g}_4 = (1/\sqrt{2})(0\,-1\,1)^{\text{T}}$, $\mathbf{g}_5 = (1/\sqrt{2})(1\,1\,0)^{\text{T}}$, and $\mathbf{g}_6 = (1/\sqrt{2})(-1\,1\,0)^{\text{T}}$. The mean conductivity (MC) is defined as follows to evaluate tissue conductivity without consideration of anisotropy:

$$\text{MC}(\mathbf{C}) = \frac{\sigma_{xx} + \sigma_{yy} + \sigma_{zz}}{3} = \frac{\lambda_1 + \lambda_2 + \lambda_3}{3} \tag{8}$$

where λ_1, λ_2, and λ_3 are the eigenvalues of the conductivity tensor. The MC represents an averaged conductivity between three principal axes. In addition, the fractional anisotropy (FA) is defined as an index of the degree of tissue anisotropy in conductivity:

$$\text{FA}(\mathbf{C}) = \sqrt{\frac{3}{2} \frac{\sum_{i=1}^{3} (\lambda_i - \text{MC}(\mathbf{C}))^2}{\sum_{i=1}^{3} \lambda_i^2}} \tag{9}$$

The FA has a value between 0 and 1. A completely isotropic tissue has an FA value of 0. Several other anisotropy indexes have been proposed such as the relative anisotropy [Basser and Pierpaoli, 1996] and the volume ratio [Basser, 1997]. Considering a report that the FA has a better signal-to-noise ratio compared to other indexes [Hasan et al., 2004], this study uses the FA for evaluating anisotropy.

METHODS

Studies were conducted under guidelines for the use and care of laboratory animals and were approved by the Institutional Animal Care and Use Committee of the University of Tokyo. Ten normal male Wistar rats (393 ± 51 g) were anesthetized with urethane (1.5 g/kg). The femoral artery and the femoral vein were catheterized to obtain blood samples for blood gas analysis and to administer drugs. The rats were tracheotomized and artificially ventilated with a 90/10% air/oxygen gas mixture at 3.5 cc, 80 cycles/min. To minimize motion artifacts, the rats were paralyzed with pancuronium bromide (0.5 mg/kg/h). Warm water was circulated between an animal cradle located in the MRI magnet and an external heater. The water temperature was 37 °C at the cradle. We checked a rectal thermometer at intervals during the measurements to confirm that the body temperatures of animals were approximately 37 °C. Blood samples were obtained to measure pH, pO_2, and pCO_2 at intervals of 1 h via a femoral arterial catheter. The conditions of artificial ventilation were readjusted, if necessary, to maintain the blood gas parameters.

Experiments were performed using the 4.7 T UNITY *INOVA* imaging spectrometer (Varian Associates, Palo Alto, CA) equipped with gradients of up to 60 mT/m. A quadrature volume coil with a 66 mm inner diameter was used for transmission and reception of signals. We performed two different measurements as described below. Five animals were used in each experiment.

The first measurement aimed to precisely estimate conductivity values in two selected voxels in the brain. The STEAM sequence was used to obtain signals from localized regions in the brain [Merboldt et al., 1993]. Two voxels with dimensions of $2\,\text{mm}^3 \times 2\,\text{mm}^3 \times 2\,\text{mm}^3$ and $1\,\text{mm}^3 \times 2\,\text{mm}^3 \times 4\,\text{mm}^3$ were located on the somatosensory cortex and the corpus callosum, respectively, as shown in Figure 1a. The acquisition parameters were as follows: repetition time $T_R = 1500$ ms, echo time $T_E = 70$ ms, mixing time $T_M = 15$ ms. The MPG was applied with pulse width $\delta = 25$ ms and pulse separation $\Delta = 50$ ms. The amplitude of the MPG was arrayed as 0, 7.33, . . ., 56.74 mT/m which corresponded to b factors of 0, 100, . . ., 6000 s/mm^2. The MPGs were applied in six directions for each amplitude. The signal-to-noise ratio was improved by averaging over 16 repetitive acquisitions. The acquisition time was 341 min. Equation (4) was

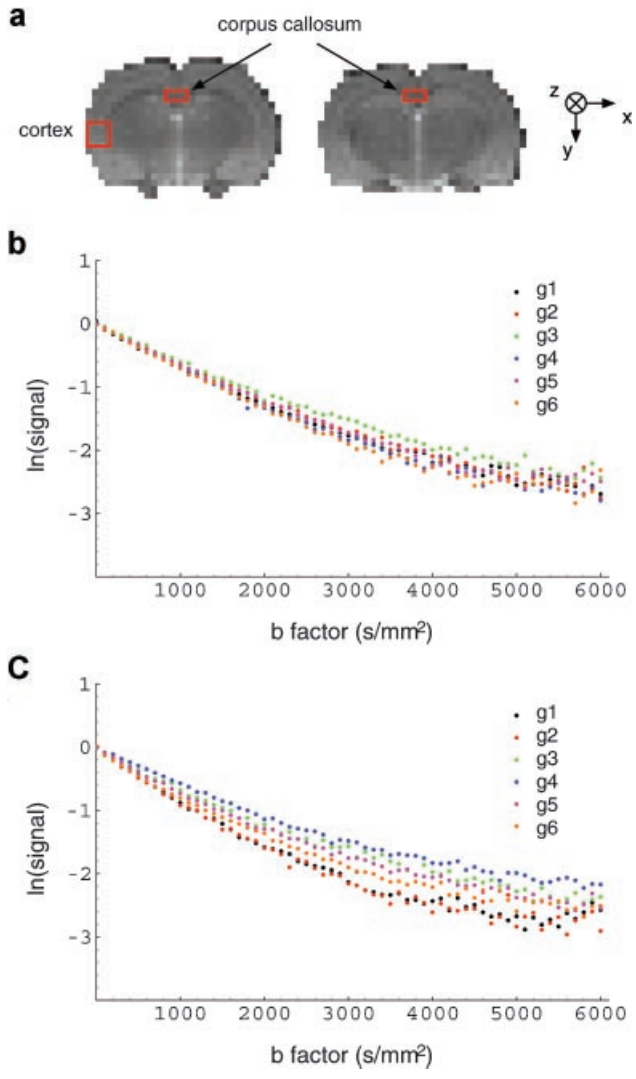

Fig. 1. **a**: Positions of voxels in the right somatosensory cortex and the corpus callosum. The two slices are adjacent to each other. **b**: Diffusion attenuation in the cortex measured by the STEAM sequence. The signals were obtained with MPGs in the following directions: $\mathbf{g}_1 = (1/\sqrt{2})(1\,0\,1)^T$, $\mathbf{g}_2 = (1/\sqrt{2})(-1\,0\,1)^T$, $\mathbf{g}_3 = (1/\sqrt{2})(0\,1\,1)^T$, $\mathbf{g}_4 = (1/\sqrt{2})(0\,-1\,1)^T$, $\mathbf{g}_5 = (1/\sqrt{2})(1\,1\,0)^T$, $\mathbf{g}_6 = (1/\sqrt{2})(-1\,1\,0)^T$. **c**: Diffusion attenuation in the corpus callosum. The MPGs were applied in the same directions as (b). [The color figure for this article is available online at www.interscience.wiley.com.]

fitted to the measured signals using the Marquardt–Levenberg algorithm [Marquardt, 1963] assuming two tensor components. The diffusion tensor parameters ($\mathbf{D}_{fast}$, $\mathbf{D}_{slow}$, and f_{fast}) were then determined. The coefficient of determination (R^2) was reported for evaluating the goodness-of-fit. These analyses were carried out using a nonlinear regression package implemented in the Mathematica software (Wolfram Research, Champaign, IL). The conductivity tensor was calculated using Equation (7). Then, the tensor invariants were calculated using Equations (8) and (9).

The second experiment aimed to investigate the spatial distribution of conductivity in the brain. Diffusion-weighted images of the rat brain were obtained in two adjacent coronal slices. The images were acquired using a spin-echo imaging sequence with acquisition parameters TR = 1500 ms, TE = 75 ms, and slice thickness = 2 mm. The MPGs were positioned on either side of the refocusing pulse with pulse width $\delta = 27$ ms and pulse separation $\Delta = 33$ ms. The images had a field-of-view (FOV) of 32 mm^2 × 32 mm^2, a data matrix of 64 × 64, and an in-plane resolution of 500 μm. The amplitude of the MPG was arrayed as 0, 34.61, 48.95, and 59.95 mT/m which corresponded to b factors of 0, 1500, 3000, and 4500 s/mm^2. The MPGs were applied in six directions, providing a total of 19 images. The acquisition time was 384 min. The signal-to-noise ratio was improved by averaging over four repetitive acquisitions for $b = 0$ and 1500 s/mm^2, and 16 repetitive acquisitions for $b = 3000$ and 4500 s/mm^2. The conductivity tensor and its invariants were calculated from the images.

Analysis of diffusion-tensor MRI of the gray matter is easily affected by a partial volume effect from the white matter or the cerebrospinal fluid (CSF). In this article, signals from the CSF were suppressed using a relatively short TR (1500 ms). The regions-of-interest (ROIs) for the gray matter were selected from regions with FA values lower than 0.2 in the FA map, while the ROIs for the white matter were selected from regions with FA values higher than 0.5.

Student's t-tests were carried out for comparing results. Differences of $P < 0.05$ were regarded as statistically significant. Data were presented as mean ± SD.

RESULTS

Figure 1b,c shows the signal intensities in the cortex and the corpus callosum which were measured using the STEAM sequence. The signals gradually decreased with an increase of the b factor. As in the previously reported experimental results obtained with high b values [Niendorf et al., 1996; Clark and Le Bihan, 2000; Clark et al., 2002; Sano et al., 2003; Maier et al., 2004], linear relations were not observed between the logarithm of the signal intensity and the b factor. In Figure 1b,c, the corpus callosum exhibited slightly higher anisotropy in the signal attenuation. Table 1 shows the eigenvalues of the fast diffusion tensor ($\mathbf{D}_{fast}$) and the slow diffusion tensor ($\mathbf{D}_{slow}$), and the fraction of the fast component (f_{fast}) obtained in the cortex and the corpus callosum. The corpus callosum had higher eigenvalues of the fast and slow diffusion tensors compared to the cortex ($P < 0.01$ for the first and second

TABLE 1. Biexponential Diffusion Parameters in the Cortex and the Corpus Callosum Obtained From the Signal Attenuations in Figure 1

f_{fast}	Eigenvalues of $\mathbf{D}_{fast}$ ($\times 10^{-3}$ mm^2/s)	Eigenvalues of $\mathbf{D}_{slow}$ ($\times 10^{-3}$ mm^2/s)	R^2
Cortex			
0.83 ± 0.06	1.08 ± 0.15	0.22 ± 0.08	0.997 ± 0.002
	0.77 ± 0.05	0.16 ± 0.05	
	0.67 ± 0.05	0.12 ± 0.04	
Corpus callosum			
0.78 ± 0.08	1.50 ± 0.27	0.30 ± 0.05	0.996 ± 0.003
	1.03 ± 0.10	0.22 ± 0.03	
	0.76 ± 0.17	0.11 ± 0.07	

The coefficient of determination (R^2) was calculated for evaluating the goodness-of-fit. The values are presented as mean $\pm$ SD in five measurements.

eigenvalues of $\mathbf{D}_{fast}$, $P < 0.05$ for the second eigenvalue of $\mathbf{D}_{slow}$, and no statistical significance for the other eigenvalues). The average of the three eigenvalues of the fast diffusion tensors in the cortex and the corpus callosum were 0.84×10^{-3} and 1.10×10^{-3} mm^2/s, respectively. A significant difference was not observed between the fast component fractions in the cortex and the corpus callosum. The fast fractions in the cortex and the corpus callosum were 0.83 and 0.78, respectively. This result indicates that the fraction of the fast component is higher than the fraction of the slow component ($P < 0.001$ for both the cortex and the corpus callosum), which is consistent with the previously reported results [Clark and Le Bihan, 2000; Clark et al., 2002; Maier et al., 2004]. Table 2 shows the eigenvalues of the conductivity tensor, the MC, and the FA. The MCs in the cortex and the corpus callosum were 0.52 and 0.62 S/m, respectively, while the FAs were 0.25 and 0.33, respectively. Both the MC and FA exhibited higher values in the corpus callosum ($P < 0.05$). The high value of FA in the corpus callosum was attributed to highly anisotropic cellular structures with neuronal axons.

Images of the fast diffusion tensor and the fraction of the fast component were constructed from diffusion-weighted images. Figure 2a–c shows images of the eigenvalues of the fast diffusion tensor. Figure 2d shows the average of the three eigenvalues of the fast diffusion tensor. The eigenvalues of the corpus callosum were higher than those of the cortex, which were consistent with the results obtained by the STEAM measurement. The white matter tissues exhibited higher anisotropy in the fast diffusion component compared to the gray matter tissues. The image of the fast component fraction (f_{fast}) is shown in Figure 2e. Figure 3a–c shows the images of the eigenvalues of the conductivity tensor. The white matter tissues had higher conductivity values and higher anisotropy compared to the gray matter tissues. The conductivity images exhibited high intensity in the white matter tissues when the MPG was applied in the same direction as the orientation of neuronal fibers. The MC image and the FA image were calculated by using Equations (8) and (9), respectively, as shown in Figures 3d,e. The MC was high in the corpus callosum and the ventricle, while the FA was high in the corpus callosum, the internal capsule, and the trigeminal nerve [see Paxinos and Watson, 1998, for the anatomy of the rat brain].

DISCUSSION

In this article, conductivity distribution in the brain was visualized using diffusion-weighted images with high b values. Measurement of conductivity distribution in the brain is important for investigations of brain function and various analyses in biomedical engineering. Neuronal electrical activity generates external electromagnetic fields. Brain activity can be investigated through measurements of electric potentials or magnetic fields by multiple detectors on the

TABLE 2. Eigenvalues of the Conductivity Tensor, the Mean Conductivity (MC), and the Fractional Anisotropy (FA) in the Cortex and the Corpus Callosum

	λ_1	λ_2	λ_3	MC	FA
Cortex (S/m)	0.67 ± 0.05	0.48 ± 0.05	0.42 ± 0.05	0.52 ± 0.04	0.25 ± 0.07
Corpus callosum (S/m)	0.85 ± 0.11	0.59 ± 0.06	0.43 ± 0.06	0.62 ± 0.06	0.33 ± 0.03

The values were calculated from the diffusion parameters in Table 1. The MC represents an averaged conductivity between three principal axes of the conductivity tensor. The FA indicates the degree of tissue anisotropy in conductivity.

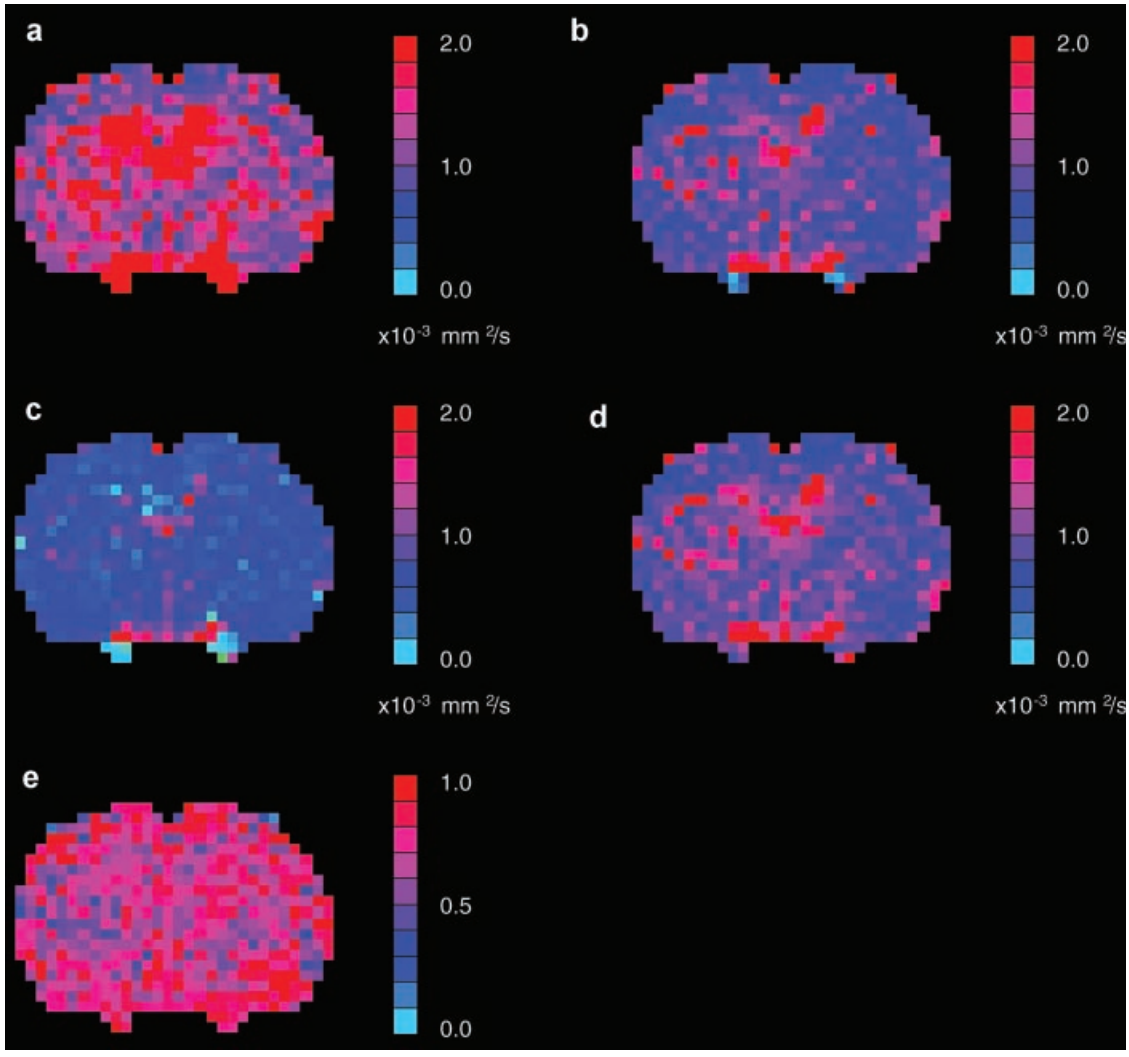

Fig. 2. **a**–**c**: Images of the three eigenvalues of the fast diffusion tensor. **d**: Image of an average of the three eigenvalues. **e**: Image of the fraction of the fast component. [The color figure for this article is available online at www.interscience.wiley.com.]

surface of the head. The three-dimensional spatial distribution of the underlying currents can be estimated from the measured electromagnetic fields through a model-based inversion procedure. Modeling studies have shown that the external electromagnetic fields are highly sensitive to the conductivity inhomogeneity and anisotropy of tissue [Zhou and van Oosterom, 1992; Haueisen et al., 1997]. Lack of knowledge regarding the conductivity distribution of the tissue can result in significant mischaracterization of the underlying currents. However, it has been difficult to investigate the inhomogeneity and anisotropy in detail by methods based on the application of electric current from surface electrodes. Thus, most of the current source estimations and analyses of electric currents in the brain have been performed on the assumption that the brain is a homogeneous and isotropic conductor [Sekino and Ueno, 2002]. The conductivity tensor images obtained in this study enable us to have a more accurate estimation of electric currents in the brain. In addition, the conductivity images could be used in numerical simulations of current distributions arising from electric or magnetic stimulations. Butson et al. [2006] used diffusion tensor MRI for incorporating the inhomogeneity and anisotropy of conductivity in numerical simulations of deep brain stimulation.

Since migrating ions encounter high resistance from cell membranes, tissue conductivity highly depends on the shape of cells, which results in the inhomogeneity and anisotropy of tissue conductivity. The results in this study indicate that white matter has higher values of conductivity and higher anisotropy in conductivity compared to gray matter. This finding suggests that, as reported in numerous articles, neuronal

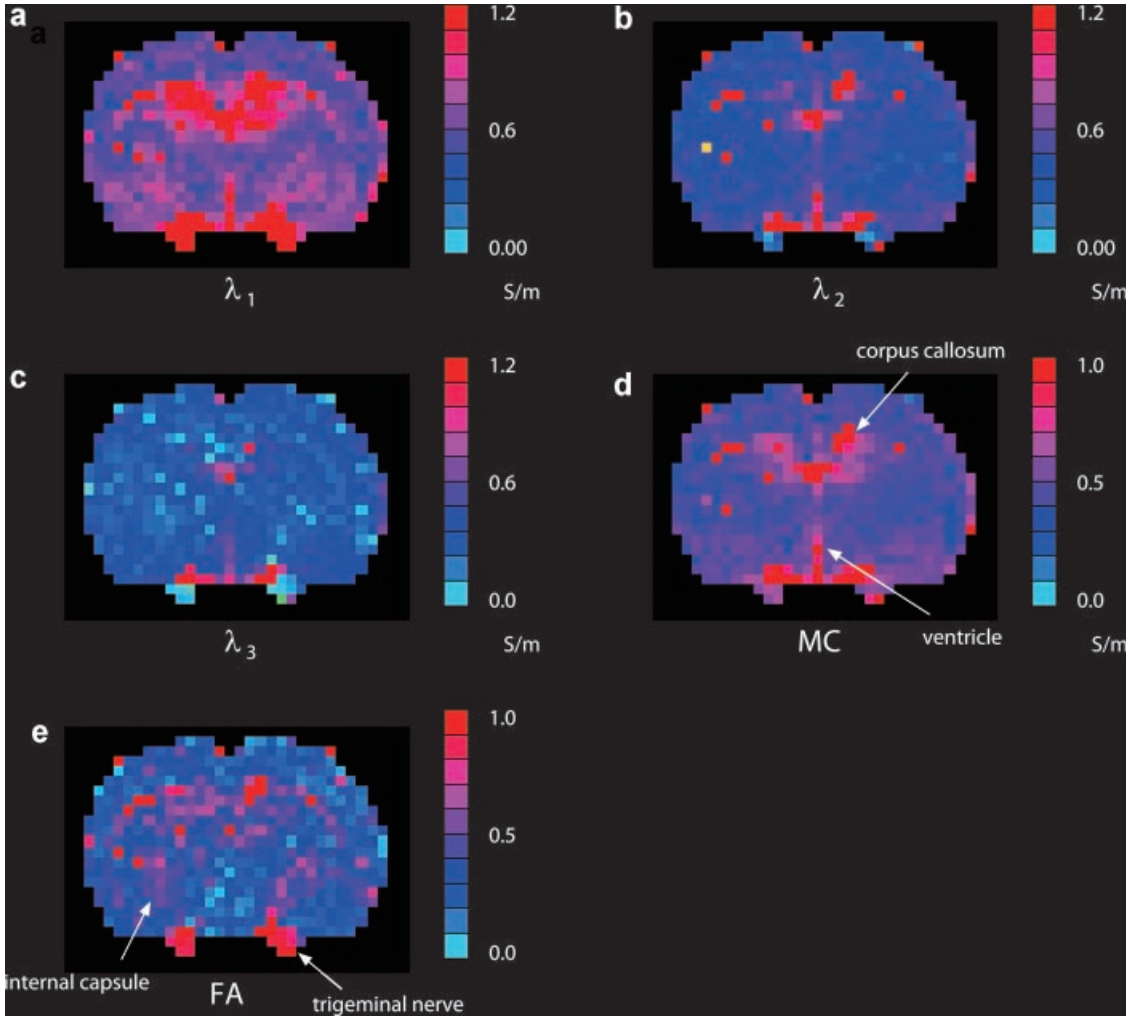

Fig. 3. **a**–**c**: Images of the conductivity in the six MPG directions. Tissues exhibited high conductivity when the MPG was applied in the same direction as the orientation of neuronal fibers. **d**: The mean conductivity (MC) image and **e**: the fractional anisotropy (FA) image. The MC was high in the corpus callosum and the ventricle, while the FA was high in the corpus callosum, the internal capsule, and the trigeminal nerve. [The color figure for this article is available online at www.interscience.wiley.com.]

fibers in white matter orient to a specific direction. However, the values presented in this article have been estimated from our conductivity model. Our finding is a consequence of our model, not a result inferred by experimental tests.

Conductivities of brain tissues have been obtained from direct measurements in which electric potentials are recorded by surface electrodes during an application of electric current of known intensity (or electric currents are recorded during an application of electric potential of known intensity). For decades, conductivity values of brain tissues at low frequencies have been reported by several groups [Freygang and Landau, 1955; Ranck, 1963; van Harreveld et al., 1963; Nicholson, 1965; Hoeltzell and Dykes, 1979; Stoy et al., 1982]. The values presented in these articles range from 0.098 S/m in white matter at 1 kHz to 0.55 S/m in gray matter at 10 Hz, suggesting little confidence in low-frequency conductivity. More recently, Gabriel and Gabriel [1996] measured and summarized conductivity values of various tissues, and this database is now widely accepted for use in dosimetry and various biomedical applications. In their report, the conductivity values of gray matter and white matter were estimated to be 0.1 and 0.06 S/m, respectively, at the low-frequency limit (below 100 Hz). Akhtari et al. [2006] measured conductivities and ADC values of excised cerebral cortex in epilepsy surgery patients, and found a negative correlation between these two quantities. This result seems to disagree with our model

and other relevant articles [Verheul et al., 1994; Wang et al., 2008]. The authors pointed out that the patients had intracranial pathologies that likely changed the cytoarchitecture of the affected brain areas, and thus altered conductivity and ADC value. The conductivity values obtained in this study are close to the highest one in the above literature, yet having more than fivefold deviation from the Gabriel's estimation. In our previous studies, we reported conductivity values for the rat brain and the human brain [Sekino et al., 2003, 2005], which also have deviations from the results of this study. We have more confidence in the values presented in this article than in the previous ones because the larger number of data points in this study, regarding both b values and MPG directions, should have resulted in smaller errors in the fitting process. However, the overall comparisons suggest that our MRI method still needs to be improved in terms of accuracy, especially if the Gabriel's estimations are reasonable.

Conductivity in biological tissues depends on frequency because electric charges in tissues are transferred by multiple mechanisms such as the migration of ions, capacitance of membranes, and rotation of polar molecules. Low-frequency currents are mainly conducted via the migration of ions, and conductivity decreases with a decrease in frequency. At frequencies ranging from 10 Hz to 100 kHz, for instance, Gabriel and Gabriel [1996] reported conductivities from 0.025 S/m to almost 0.08 S/m for white matter and from 0.035 S/m to about 0.13 S/m for gray matter. In this article, conductivity was estimated assuming that charges are transferred only by ion migration, ignoring capacitive currents through cell membranes and conductive currents in intracellular spaces. This model explains electric conductions at the low-frequency limit. The conductivity calculated from the ADC therefore corresponds to the value at this limit (below 100 Hz). Neuronal electrical activities typically have such low-frequency components. For instance, the major component of spontaneous pseudoperiodic alpha wave is on the order of 10 Hz [Cohen, 1968]. Therefore, the results of conductivity imaging are potentially applicable to the reconstruction of electric and magnetic sources from electroencephalogram and magnetoencephalogram. Anisotropy in tissue conductivity is generally only expected at fairly low frequencies, where ions may reach various membranes in one half-cycle. For example, the anisotropy of muscle tissue (consisting of very long, thin cells and parallel membranes) disappears by the low MHz regime [Gabriel and Gabriel, 1996]. To obtain tissue conductivity for higher frequencies using MRI, construction of a new model is necessary. A conductivity model for higher frequency would consider, as a first approximation, an increase in the contribution from intracellular space, which can be estimated from the slow component of ADC. In addition, the capacitance of the cell membrane needs to be addressed because charge and discharge of the cell membrane significantly contribute to electric conduction in tissues. The intracellular contribution depends on the capacitance of the cell membrane.

In this article, the effective conductivity of tissue was calculated from the conductivity of extracellular fluid using Equation (1). This equation was originally derived for two-phase isotropic media with spherical inclusions. Several other equations have been proposed for anisotropic media with ellipsoidal inclusions [Sen et al., 1981; Lu, 1998; Shafiro and Kachanov, 2000]. Sen et al. [1981] formulated the effective conductivity (σ_a) for ellipsoidal inclusions with principal axes a, b, and c, and with an electric field applied along the a-axis:

$$\sigma_a = \frac{(1 - L_a)\phi}{1 - \phi L_a}\sigma_{\text{ext}} \tag{10}$$

where L_a is the depolarizing factor:

$$L_a = \frac{1}{2}\text{abc}\int_0^\infty \frac{\text{d}s}{(s + a^2)[(s + a^2)(s + b^2)(s + c^2)]^{1/2}} \tag{11}$$

The spherical inclusions ($a = b = c$) lead to $L_a = 1/3$. Given the porosity variable ϕ reducing to the fractional volume of the extracellular space v_{ext}, Equation (10) in this case reduces to Equation (1). Though the shape of a cell is not a perfect sphere, for simplicity we approximated the effective conductivity in tissue by Equation (1). For example, an ellipsoidal inclusion of $a = 2b = 2c$ gives $L_a = 0.174$. In the case of this inclusion with a porosity $\phi = = 0.5$, the effective conductivity calculated from Equation (1) is 88% of the effective conductivity calculated from Equation (10).

The calculation of tissue conductivity in this article is based on the model that the fast and slow components of ADC originate from the extracellular fluid and intracellular fluid, respectively. The ADC of extracellular fluid and the fractional volume of extracellular space is approximated by the fast component of ADC and the fraction of the fast component, respectively. A result of an in vitro experiment indicates that the fraction of the fast component calculated by Equation (4) has a similar value to the actual volume fraction of extracellular space [Sano et al., 2003]. However, several studies have shown that both fast and slow components arise from the intracellular space [Sehy et al., 2002]. Details of the relation between diffusion signal attenuation and tissue microstructure

remain to be understood. Further studies are required for a better understanding of the diffusion phenomena in biological tissues and for investigating the origins of the fast and slow diffusion components.

Equation (4) for compartmentalizing fast and slow diffusion tensors is based on a model in which the fractions of fast and slow components are equal in all MPG directions. On the other hand, there has been another model in which the fractions depend on the MPG direction [Maier et al., 2004]. This study uses the former model because the fractional volume of extracellular space is a direction-independent scalar quantity.

In voxels located close to the boundary between tissue and CSF, the measurement of ADC and fast/slow fractions may be affected by the partial volume effect from CSF [Falconer and Narayana, 1997]. The effect can sufficiently be suppressed using an inversion recovery method. A previous study, with the use of this technique, reported that fast component fractions of the cortex and corpus callosum were 0.73 and 0.65, respectively [Clark and Le Bihan, 2000]. In this study, we did not use the inversion recovery method. Instead, the measurements were carried out with a relatively short TR (=1500 ms) for reducing signals from CSF. This approach provided a moderate CSF suppression, and enabled us to shorten the time for measurements. As a result, the fractions of the fast component obtained in this study were 15–20% higher than the values reported in the above paper.

This study consists of two measurements: the STEAM and spin-echo imaging. The STEAM measurement purposed an improvement of accuracy in the biexponential fitting by increasing the number of steps in the b factor. On the other hand, spin-echo imaging purposed an investigation of spatial distribution of conductivity and anisotropy. Because acquisitions of images require much more time compared to the STEAM measurements, the number of steps in the b factor in the imaging study is limited. The use of echo planar imaging (EPI) would enable us to achieve both the accuracy of fitting and the investigation of spatial distribution, though we could not use it in this study because of severe image distortions. The EPI measurement can be performed with a large number of signal averages, and the final signal to noise ratio of EPI would be higher than that of the standard spin echo sequence. For instance, if the number of averages is increased by a factor of 64, the signal-to-noise ratio can be improved by a factor of up to 8.

The MC obtained by the STEAM was approximately 20% higher than the MC calculated in the pixels of image corresponding to the cortex. The FA value of the cortex obtained by the STEAM (0.25) was higher than the FA value obtained by spin-echo imaging (0.16). These differences can be partially explained by the differences in the b factor and the diffusion time ($\Delta - \delta/3$) in each measurement.

This study gave an FA value of 0.33 for the corpus callosum, which is significantly lower than the reported FA values of approximately 0.7 for the human corpus callosum [Clark et al., 2002; Maier et al., 2004]. This difference is attributable to a structural difference of the brain tissue between rats and humans, and the partial volume effect from the gray matter and the CSF.

Although this article focused on the conductivity of the brain due to its particular importance in biomedical engineering, this method of obtaining conductivity from the ADC can be applied, in principle, to any tissue. Since brain tissue has a small ADC compared to other tissues such as muscle and fat, signal attenuation of brain tissue by an applied MPG is relatively small. The MPG significantly decreases the signal intensities of tissues with a high ADC. Bone tissue exhibits a low signal because of its long T_1 relaxation time and short T_2 relaxation time. Conductivity imaging of tissues other than the brain has not yet succeeded under the experimental conditions of this study. However, because recently developed rapid scan techniques allow for an increase in the number of averages, it may be possible to obtain conductivity distributions of bone and other tissues by the same procedure.

There is a possibility that exposure to the RF and magnetic fields from MRI procedure might affect the conductivity of brain tissue. Equation (6) indicates for the first approximation that conductivity is inversely proportional to the temperature of tissue. If the magnitude of RF is strong enough to increase the temperature, conductivity would slightly decrease. In addition, a number of previous studies have provided evidences that exposure to static magnetic field causes a variety of biological effects, which raises the question of whether the exposure affects the conductivity or not. These issues are beyond the scope of this article, and we leave them for future works.

It has been difficult to investigate the anisotropy in conductivity by conventional imaging methods even though highly anisotropic conductivity is expected in the brain due to the fibrous nature of the neurons. This new method based on MRI has high spatial resolution and less invasiveness compared to conventional methods such as EIT, and the surrounding tissues do not affect measurements. Moreover, this new method of obtaining conductivity distributions from the ADC can easily visualize the distribution of conductivity anisotropy.

REFERENCES

Akhtari M, Salamon N, Duncan R, Fried I, Mathern GW. 2006. Electrical conductivities of the freshly excised cerebral cortex in epilepsy surgery patients; correlation with pathology, seizure duration, and diffusion tensor imaging. Brain Topogr 18:281–290.

Atkins PW. 1998. Physical chemistry. Oxford: Oxford University Press.

Basser PJ. 1997. New histological and physiological stains derived from diffusion-tensor MR images. Ann N Y Acad Sci 820: 123–138.

Basser PJ, Pierpaoli C. 1996. Microstructural and physiological features of tissues elucidated by quantitative-diffusion-tensor MRI. J Magn Reson B 111:209–219.

Butson CR, Cooper SE, Henderson JM, McIntyre CC. 2006. Predicting the effects of deep brain stimulation with diffusion tensor based electric field models. Med Image Comput Comput Assist Interv Int Conf Med Image Comput Comput Assist Interv 9:429–437.

Clark CA, Le Bihan D. 2000. Water diffusion compartmentation and anisotropy at high b values in the human brain. Magn Reson Med 44:852–859.

Clark CA, Hedehus M, Moseley ME. 2002. In vivo mapping of the fast and slow diffusion tensors in human brain. Magn Reson Med 47:623–628.

Cohen D. 1968. Magnetoencephalography: Evidence of magnetic fields produced by alpha-rhythm currents. Science 161:784–786.

Cole KS, Li CL, Bak AF. 1969. Electrical analogues for tissues. Exp Neurol 24:459–473.

Falconer JC, Narayana PA. 1997. Cerebrospinal fluid-suppressed high-resolution diffusion imaging of human brain. Magn Reson Med 37:119–123.

Freygang WH, Jr., Landau WM. 1955. Some relations between resistivity and electrical activity in the cerebral cortex of the cat. J Cell Physiol 45:377–392.

Gabriel C, Gabriel S. 1996. Compilation of the dielectric properties of body tissues at RF and microwave frequencies. Available from: http://niremf.ifac.cnr.it/docs/DIELECTRIC/home.html.

Geddes LA, Baker LE. 1967. The specific resistance of biological material—A compendium of data for the biomedical engineer and physiologist. Med Biol Eng 5:271–293.

Hasan KM, Parker DL, Alexander AL. 2001. Comparison of gradient encoding schemes for diffusion-tensor MRI. J Magn Reson Imaging 13:769–780.

Hasan KM, Alexander AL, Narayana PA. 2004. Does fractional anisotropy have better noise immunity characteristics than relative anisotropy in diffusion tensor MRI? An analytical approach. Magn Reson Med 51:413–417.

Haueisen J, Ramon C, Eiselt M, Brauer H, Nowak H. 1997. Influence of tissue resistivities on neuromagnetic fields and electric potentials studied with a finite element model of the head. IEEE Trans Biomed Eng 44:727–735.

Hoeltzell PB, Dykes RW. 1979. Conductivity in the somatosensory cortex of the cat—Evidence for cortical anisotropy. Brain Res 177:61–82.

Jones DK, Horsfield MA, Simmons A. 1999. Optimal strategies for measuring diffusion in anisotropic systems by magnetic resonance imaging. Magn Reson Med 42:515–525.

Kataoka H, Eguchi T, Masui H, Miyakubo K, Nakayama H, Nakamura N. 2003. Scaling relation between electrical conductivity percolation and water diffusion coefficient in sodium bis(2-ethylhexyl) sulfosuccinate-based microemulsion. J Phys Chem B 107:12542–12548.

Kreuer KD, Schönherr E, Maier J. 1994. Proton and oxygen diffusion in $BaCeO_3$ based compounds: A combined thermal gravimetric analysis and conductivity study. Solid State Ionics 70:278–284.

Lu SY. 1998. Effective conductivities of aligned spheroid dispersions estimated by an equivalent inclusion model. J Appl Phys 84:2647–2655.

Maier SE, Vajapeyam S, Mamata H, Westin CF, Jolesz FA, Mulkern RV. 2004. Biexponential diffusion tensor analysis of human brain diffusion data. Magn Reson Med 51:321–330.

Marquardt DW. 1963. An algorithm for least-squares estimations of nonlinear parameters. J Soc Ind Appl Math 11:431–441.

Matherall P, Barger DC, Smallwood RH, Brown BH. 1996. Three-dimensional electrical impedance tomography. Nature 380: 509–512.

Mayer M, Brunner P, Merwa R, Smolle-Jüttner FM, Maier A, Scharfetter H. 2006. Direct reconstruction of tissue parameters from differential multifrequency EIT in vivo. Physiol Meas 27:S93–S101.

Merboldt KD, Hörstermann D, Hänicke W, Bruhn H, Frahm J. 1993. Molecular self-diffusion of intracellular metabolites in rat brain in vivo investigated by localized proton NMR diffusion spectroscopy. Magn Reson Med 29:125–129.

Merwa R, Hollaus K, Oszkar B, Scharfetter H. 2004. Detection of brain oedema using magnetic induction tomography: A feasibility study of the likely sensitivity and detectability. Physiol Meas 25:347–354.

Nicholson PW. 1965. Specific impedance of cerebral white matter. Exp Neurol 13:386–401.

Niendorf T, Dijkhuisen RM, Norris DG, van Lookeren Campagne M, Nicolay K. 1996. Biexponential diffusion attenuation in various states of brain tissue: Implications for diffusion-weighted imaging. Magn Reson Med 36:847–857.

Papadakis NG, Xing D, Huang CL, Hall LD, Carpenter TA. 1999. A comparative study of acquisition schemes for diffusion tensor imaging using MRI. J Magn Reson 137:67–82.

Paxinos G, Watson C. 1998. The rat brain. San Diego: Academic Press.

Ranck JB, Jr. 1963. Specific impedance of rabbit cerebral cortex. Exp Neurol 7:144–152.

Sano M, Sekino M, Ogiue-Ikeda M, Ueno S. 2003. Biexponential attenuation of water diffusion in leukemic cells. Proceedings of the 11th Scientific Meeting ISMRM.

Saulnier GJ, Blue RS, Newell JC, Isaacson D, Edic PM. 2001. Electrical impedance tomography. IEEE Signal Process Mag 18:31–43.

Sehy JV, Ackerman JJ, Neil JJ. 2002. Evidence that both fast and slow water ADC components arise from intracellular space. Magn Reson Med 48:765–770.

Sekino M, Ueno S. 2002. Comparison of current distributions in electroconvulsive therapy and transcranial magnetic stimulation. J Appl Phys 91:8730–8732.

Sekino M, Yamaguchi K, Iriguchi N, Ueno S. 2003. Conductivity tensor imaging of the brain using diffusion-weighted magnetic resonance imaging. J Appl Phys 93:6730–6732.

Sekino M, Inoue Y, Ueno S. 2005. Magnetic resonance imaging of electrical conductivity in the human brain. IEEE Trans Magn 41:4203–4205.

Sen PN, Scala C, Cohen MH. 1981. A self-similar model for sedimentary rocks with application to the dielectric constant of fused glass beads. Geophysics 46:781–795.

Shafiro B, Kachanov M. 2000. Anisotropic effective conductivity of materials with nonrandomly oriented inclusions of diverse ellipsoidal shapes. J Appl Phys 87:8561–8569.

Stoy RD, Foster KR, Schwan HP. 1982. Dielectric properties of mammalian tissues from 0.1 to 100 MHz: A summary of recent data. Phys Med Biol 27:501–513.

Ueno S, Iriguchi N. 1998. Impedance magnetic resonance imaging: A method for imaging of impedance distributions based on magnetic resonance imaging. J Appl Phys 83:6450–6452.

van Harreveld A, Murphy A, Nobel KW. 1963. Specific resistance of rabbit's cortical tissue. Am J Physiol 205:203–207.

Verheul HB, Balazs R, Berkelbach van der Sprenkel JW, Tulleken CAF, Nicolay K, Tamminga KS, van Lookeren Campagne M. 1994. Comparison of diffusion-weighted MRI with changes in cell volume in a rat model of brain injury. NMR Biomed 7:96–100.

Wang K, Zhu S, Mueller BA, Lim KO, Liu Z, He B. 2008. A new method to derive white matter conductivity from diffusion tensor MRI. IEEE Trans Biomed Eng 55:2481–2486.

Xu J, Li GZ, Zhang ZQ, Zhou GW, Ji KJ. 2001. A study of the microstructure of CTAB/1-butanol/octane/water system by PGSE-NMR, conductivity and cryo-TEM. Colloid Surf A 191:269–278.

Yukawa Y, Iriguchi N, Ueno S. 1999. Impedance magnetic resonance imaging with external AC field added to main static field. IEEE Trans Magn 35:4121–4123.

Zhou H, van Oosterom A. 1992. Computation of the potential distribution in a four-layer anisotropic concentric spherical volume conductor. IEEE Trans Biomed Eng 39:154–158.